

## Protective coatings based on Zr-Ti-Si-N their physical and mechanical properties and phase composition

**Abstract.** Hard and super hard coatings of Zr-Ti-Si-N of from 2.8 to 3.5  $\mu\text{m}$  thickness were fabricated using vacuum arc source with (HF) stimulation. Six series of samples with various Zr and Ti content were studied. The samples were annealed in vacuum and in air at 1200°C. It was found that films with a high Zr and Ti content were thermally stable up to 1180°C. At the same time, a thin oxide layer of 180 to 240nm was found in the surfaces, which protected the sample from destruction. A size of grains of a substitution solid solution (Zr, Ti)N varied from (10 – 12)nm to 25nm, but Ti concentration in the solid solution increased. In the process of annealing, hardness of the best series of samples increased from 39.6  $\pm$  1.4GPa to 53.6GPa, which seemed to indicate that a spinodal segregation along grain interfaces was finished. Tribotechnical characteristics of coatings were measured for various contents of basic elements Zr, Ti, and Si. The work was funded by the project of NAS of Ukraine "Nanomaterials, Nanotechnologies, Nanosystems".

**Streszczenie.** Twarde i supertwarde powłoki Zr-Ti-Si-N o grubości od 2,8 do 3,5  $\mu\text{m}$  zostały wytworzone wykorzystując próżniowe źródło łuku ze stymulacją HF. Przebadano sześć serii próbek o różnej zawartości Zr oraz Ti. Próbki zostały wygrzane w próżni i w powietrzu w temperaturze 1200°C. Wykazano, że warstwy z wysoką zawartością Zr oraz Ti były stabilne termicznie do temperatury 1180°C. W tym samym czasie cienka warstwa tlenku o grubości od 180 do 240nm została zidentyfikowana w obrębie powierzchni, które ochraniały próbkę przed zniszczeniem. Rozmiar ziaren substytutu roztworu stałego (Zr, Ti)N zmienił się od (10 – 12)nm do 25nm, jednakże koncentracja Ti w roztworze stałym wzrosła. W procesie wygrzewania twardość najlepszej serii próbek wzrosła od 39,6  $\pm$  1,4GPa do 53,6GPa, co wydaje się wskazywać, że oddzielenie spinodalne wzdłuż interfejsu ziaren zostało zakończone. Charakterystyki trybo techniczne powłok zostały zmierzone dla różnych zawartości podstawowych pierwiastków Zr, Ti, oraz Si. Badania zostały sfinansowane ze środków ukraińskiego projektu NAS „Nanomateriały, Nanotechnologie, Nanosystemy”. (Powłoki ochronne wytworzone w oparciu o Zr-Ti-Si-N – właściwości mechaniczne i skład fazowy).

**Keywords:** thermal stability, superhard coatings, nanostructured, Zr-Ti-Si-N.

**Słowa kluczowe:** stabilność temperaturowa, powłoki supertwarde, nanostruktury, Zr-Ti-Si-N.

### Introduction

Recently, nanocomposite coatings of new generation composed of at least two phases with nanocrystalline and/or amorphous structures are of great interest. Due to very small size (10 nm) of their grains and more important role of boundary zones surrounding single grains, nanocomposite materials behave unlike traditional materials with grain size higher than 100 nm and display quite different properties. Novel unique physical and functional properties of nanocomposites promote rapid development of nanocomposite materials. The purpose of this work was to study formation of superhard coatings on Zr-Ti-Si-N base and their properties including thermal stability. Also we should like to note theoretical works [1-4], which studied electron structure, stability, decohesion mechanism, shear of interfaces in superhard and heterostructures nc-TmN/ $\alpha$ -Si<sub>3</sub>N<sub>4</sub>. Therefore, the purpose of this work was to study formation of superhard coatings on Zr-Ti-Si-N base and their properties including thermal stability.

### Experimental details

Coatings were fabricated using vacuum-arc deposition from unit-cast, Zr, Zr-Si, and Zr-Ti-Si targets. Films were deposited in nitrogen atmosphere. Deposition was carried out using standard vacuum-arc and HF discharge methods. Bias potential was applied to substrate from HF generator, which produced impulses of convergent oscillations with  $\leq$  1MHz frequency, every impulse duration being 60 $\mu\text{s}$ , their repetition frequency – about 10kHz. Due to HF diode effect, value of negative autobias potential occurring in substrate increased from 2 to 3kV at the beginning of impulse (after start of discharger operation). Coatings of 2 to 3.5 $\mu\text{m}$  thickness were deposited to steel substrates (of 20 and 30mm diameter and 3 to 5mm thickness). Deposition was performed without additional substrate heating. Zr-Ti-Si-N coatings were deposited to polycrystalline steel (St.3 – 0.3wt.%C, Fe the rest). Molecular nitrogen was employed as a reaction gas (Table.1). It is cathode current in A; PN is pressure of atomic nitrogen in Pa units; URF is bias voltage

of Hf discharge; U is bias voltage under conditions of vacuum-arc discharge.

Table 1. Physical-technological parameters of deposition

Evaporated materials	Coating	Ia A	PN Pa	URF V	U V	Notes
Zr	ZrN	110	0.3	-	200	Standard technology
Zr	ZrN	110	0.3	200	-	HF deposition
Zr-Si	(ZrSi)N	110	0.3	200	-	HF deposition
Ti-Zr-Si	(Ti-Zr-Si)N	110	0.3	200	-	HF deposition

Annealing was performed in air medium, in a furnace SNOL 8.2/1100 (Kharkov, Ukraine), under temperature T = 300°C, 500°C, and 800°C, and in a vacuum furnace SNVE-1.3, under 5 x 10<sup>-4</sup>Pa pressure, and T = 300°C, 500°C and 1180°C. Studies of phase compositions and structures were performed using X-ray diffraction devices DRON-3M, under filtered emission Cu-K $\alpha$ , using secondary beam of a graphite monochromator. Diffraction spectra were taken point-by-point, with a scanning step 2 $\theta$  = 0.05 to 0.1°.

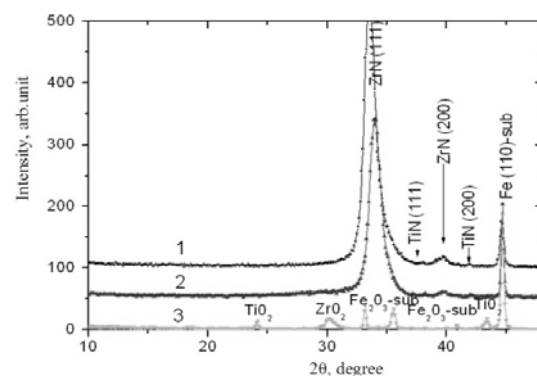


Fig.1. XRD diffraction patterns for Zr-Ti-Si target in 0.3 Pa nitrogen atmosphere (vacuum-arc source with HF discharge): 1 – for initial (as-received) samples; 2 – for annealed at 500°C (30min in vacuum); 3 – for annealed at 800°C (30min in vacuum)

## Results and discussion

Analyzing phase composition of Zr-Ti-Si-N films, we found that a basic crystalline component of as-deposition on state was solid solution (Zr, Ti)N based on cubic lattice of structured NaCl. In Table 2, we presents x-ray diffraction curves: a lattice period in non-stressed cross-section ( $a_0$ ), value of macrodeformation  $\epsilon$ , microdeformation  $\langle\epsilon\rangle$ , and concentration of packing defects  $\text{adef.pack}$ . The data were obtained both for samples after coating deposition and for those annealed in vacuum and air under various temperatures. Crystallites of solid (Zr, Ti)N solution underwent compressing elastic macrostresses occurring in a “film-substrate” system. Compressing stresses, which were present in a plane of growing film, indicated development of compressing deformation in a crystal lattice, which was identified by a shift of diffraction lines in the process of angular surveys (“ $\sin 2\psi$  – method”) and reached – 2.93% value (Table 2). With  $E \approx 400\text{GPa}$  characteristic elastic modulus and 0.28 Poisson coefficient, deformation value corresponded to that occurring under action of compressing stresses  $\sigma_c \approx - 8.5\text{GPa}$ . We should also note that such high stresses characterize nitride films, which were formed under deposition with high radiation factor, which provided high adhesion to base material and development of compression stresses in the film, which was stiffly bound to the base material due to “atomic peening”-effect.

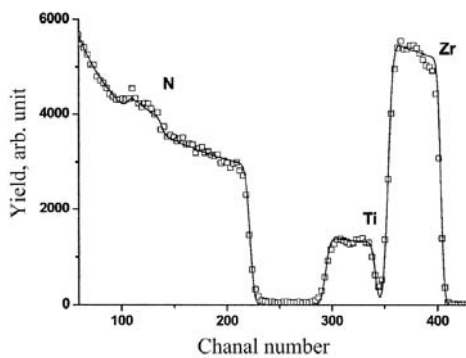


Fig.2. Energy spectrum of 1.35MeV  $\text{He}^+$  ion measured for Ti-24%, Zr-30%, N-42% nanocomposite coating; arrows indicate kinematical boundaries of elements

Qualitative changing of phase composition was observed in films under vacuum annealing at  $T_{\text{an}} > 1000^\circ\text{C}$ . Appearance of zirconium and titanium oxides was related to oxidation relaxation under coating surface interaction with oxygen atoms coming from residual vacuum atmosphere under annealing. Under annealing temperatures below  $1000^\circ\text{C}$ , coatings phase composition remained practically unchanged. One could not only changed width of diffraction lines and their shift to higher diffraction angles. The latter characterizes relaxation of compressing stresses in coatings. Changed diffraction lines were related to increased crystalline sizes (in general) and decreased micro-deformation. In Zr-Ti-Si-N coatings, increased Ti concentration, formation of three phases- (Zr, Ti)N-nc-57vol.%, TiN-nc-35vol.%, and  $\alpha - \text{Si}_3\text{N}_4 \geq 7.5 \text{ vol.}\%$ , as well as changes of grain size, which decreased to (6 to 8)nm in (Zr, Ti)N and (10 to 12) in TiN in comparison with first series resulted in increased nanohardness and decreased difference in hardness values. Annealing in vacuum below  $500^\circ\text{C}$  finished the process of spinodal segregation at grain boundaries and interfaces. Annealing stimulated segregation processes and formed stable modulated coating structure [1,4,8]. X-ray diffraction spectra taken for the coatings of Zr-Ti-Si-N system after deposition. The relative intensities of peaks indicate amorphous  $\beta\text{-Si}_3\text{N}_4$ ,  $\alpha$ -

Fe phase crystallites and metallic sublattice of (Zr, Ti)N solid solution.

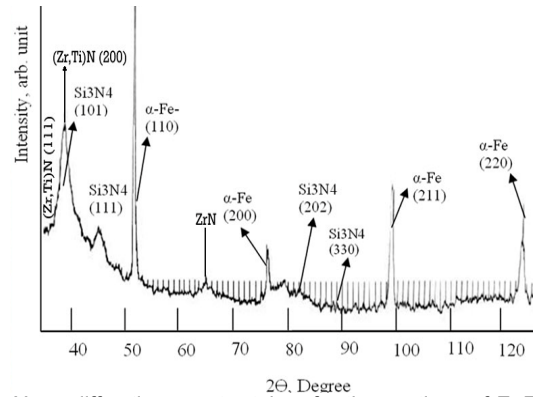


Fig.3. X-ray diffraction spectra taken for the coatings of Zr-Ti-Si-N system after deposition

Figure 4 shows scratch properties of Zr-Ti-Si-N. The friction coefficient ( $\mu$ ) between two solid surfaces is defined as the ratio of the tangential force ( $F$ ) required to produce sliding divided by the normal force between the surfaces ( $N$ ). Normal force  $F_n$  (occasionally  $N$ ) is the component, perpendicular to the surface of contact, of the contact force exerted on an object by the surface. Acoustic Emission is a naturally occurring phenomenon whereby external stimuli, such as mechanical loading, generate sources of elastic waves. Penetration Depth is a measure of how deep light or any electromagnetic radiation can penetrate into a material. It is defined as the depth at which the intensity of the radiation inside the material falls to  $1/e$  (about 37%) of its original value at (or more properly, just beneath) the surface.

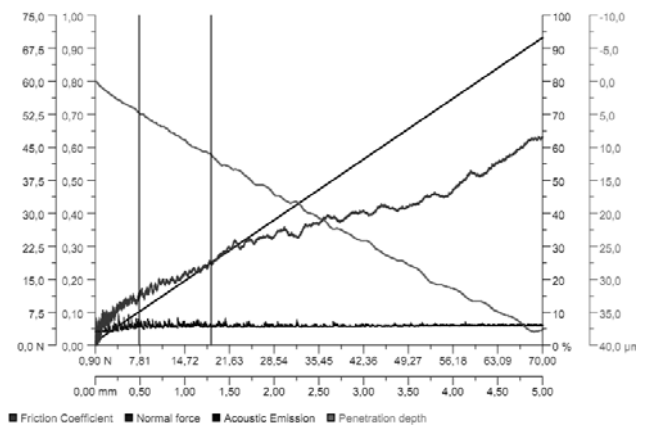


Fig.4. Scratch properties of Zr-Ti-Si-N: friction coefficient, normal force, acoustic emission, penetration depth

## Conclusions

In such a way, decreased concentration of active oxygen atoms coming from annealing atmosphere increased stability of film phase composition from  $500$  to  $1000^\circ\text{C}$ . High macro- and microdeformation occurring in the coating seems to be related to an “atomic peening” effect resulting to non-ordered distribution of titanium atoms implanted to the film during its growth. In the course of annealing, the macro- and micro-deformation relaxed. The relaxation was accompanied by formation of deformation packing defects in a metallic sublattice of (Zr, Ti)N solid solution. This can be revealed by X-ray scanning, which demonstrated shift and broadening of diffraction peaks. Highest content of packing defects indicated shift of most closely packed planes in a fcc-sublattice (111) with respect to each other

[8-11] and became pronounced under vacuum annealing at  $T_{an} = 800$  to  $1100^{\circ}\text{C}$  reaching 15.5vol.%. In Zr-Ti-Si-N coatings, increased Ti concentration, formation of three phases- (Zr, Ti)N-nc-57vol.%, TiN-nc-35vol.%, and  $\alpha - \text{Si}_3\text{N}_4 \geq 7.5$  vol.%, as well as changes of grain size, which decreased to (6 to 8)nm in (Zr, Ti)N and (10 to 12) in TiN in comparison with first series resulted in increased

nanohardness and decreased difference in hardness values. Annealing in vacuum below  $500^{\circ}\text{C}$  finished the process of spinodal segregation at grain boundaries and interfaces. Annealing stimulated segregation processes and formed stable modulated coating structure [1, 4, 8].

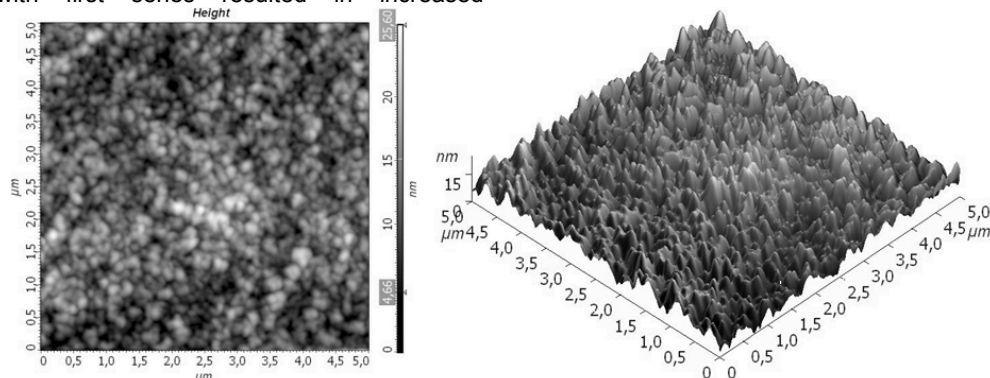


Fig.5. Surface morphology of coatings (Zr-Ti-Si)N with  $U = -150$  V,  $P = 0,8$  Pa

Table 2. Changes of structure and substructure parameters occurring in ion-plasma deposited films of Zr-Ti-Si-N system in the course of high-temperature annealing in vacuum and in air

Parameters of structure	After deposition	$T_{an}=300^{\circ}\text{C}$ vacuum	$T_{an}=500^{\circ}\text{C}$ vacuum	$T_{an}=1100^{\circ}\text{C}$ vacuum	$T_a=300^{\circ}\text{C}$ air	$T_{an}=500^{\circ}\text{C}$ air
$a_0$ , nm	0,45520	0,45226	0,45149	0,45064	0,45315	0,45195
$\epsilon$ , %	-2,93	-2,40	-1,82	-1,09	-2,15	-1,55
$\langle \epsilon \rangle$ , %	1,4	1,0	0,85	0,8	0,95	0,88
$\alpha_{def. pack.}$	0,057	0,085	0,107	0,150	0,090	0,128

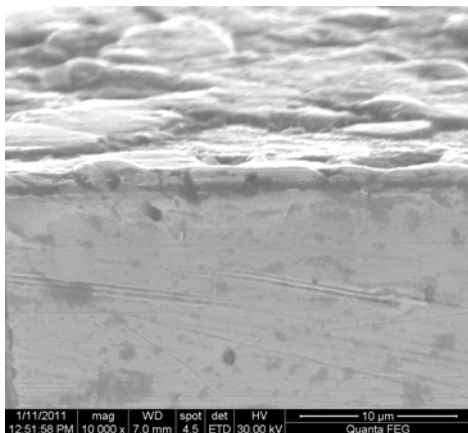


Fig.6. Cross-section of hard coating Zr-Ti-Si-N (high concentration of Si and N)

#### REFERENCES

- [1] Pogrebnjak A.D., Ruzimov Sh.M., Alontseva D.L., Zukowski P., Karwat C., Kozak C., Kolasik M., Structure and properties of coatings on Ni base deposited using a plasma jet before and after electron a beam irradiation, *Vacuum*, 81 (2007), n. 10, 1243-1251
- [2] Pogrebnjak A.D., Danilionok M.M., Uglov V.V., Erdybaeva N., Kirik G., Dub S., Rusakov V., Shpylenko A., Zukovski P., Tuleushev Y., Nanocomposite protective coatings based on Ti-N-Cr/Ni-Cr-B-Si-Fe, their structure and properties, *Vacuum*, 83 (2009), n. 1, 235-239
- [3] Misaelides P., Hadzidimitrpu A., Noly.F., Pogrebnjak A.D., Tyurin Y.N., Kosionidis S., Preparation, characterization, and corrosion behavior of protective coatings on stainless steel samples deposited by plasma detonation techniques, *Surf. And Coat. Tech.*, 180-181 (2004), 290-296

- [4] Pogrebnjak A.D., Kulmenteva O.P., Kobzev A.V., Tyurin Yu.N., Golovenko S.I., Boiko A.G., Mass transfer and doping during electrolyte-plasma treatment of cast iron, *Tech. Phys. Lett.*, 29 (2004), n. 4, 312-315
- [5] Pogrebnjak A.D., Bazyl E.A., Modification of wear and fatigue characteristics of Ti-V-Al alloy by Cu and Ni ion implantation and high-current electron beam treatment, *Vacuum*, 64 (2001), n. 1, 1-7
- [6] Pogrebnjak A.D., Ilyashenko M.V., Kulmenteva O.P., Kshnjakin V.S., Kobzev A.P., Tyurin Y.N., Kolisnichenko O., Structure and properties of  $\text{Al}_2\text{O}_3$  and  $\text{Al}_2\text{O}_3+\text{Cr}_2\text{O}_3$  coatings deposited to steel 3 (0.3 wt%C) substrate using pulsed detonation technology, *Vacuum*, 62 (2001), n. 1, 21-26
- [7] Pogrebnjak A.D., Lebed A.G., Ivanov Yu.F., Modification of single crystal stainless steel structure (Fe-Cr-Ni-Mn) by high-power ion beam, *Vacuum*, 63 (2001), n. 4, 483-486
- [8] Pogrebnjak A.D., Kobzev A.V., Gritsenko B.P., Sokolov S., Bazyl E., Sviridenko N.V., Valyaev A.N., Ivanov Y.F., Effect of Fe and Zr ion implantation and high-current electron irradiation treatment on chemical and mechanical properties of Ti-V-Al alloy, *J. Appl. Phys.*, 87 (2000), n. 5, 2142-2148
- [9] Lavrentiev V.I., Pogrebnjak A.D., High-dose ion implantation into metals, *Surf. And Coat. Tech.*, 99 (1998), n. 2, 24-32

**Author:** Ph.D. Grigori V.Kiryk, Sumy State University, 2, R-Korsakov Str., 40007, Sumy, Ukraine, E-mail: alexp@i.ua  
Ph.D., Eng. Czesław Kozak, Lublin University of Technology, 38a Nadbystrzycka Str., 20-618 Lublin, Poland  
Prof. Marek Opielak, Lublin University of Technology, 38 Nadbystrzycka Str., 20-618 Lublin, Poland